Electronic Supplementary Information (SI) for

Versatile Cl-decorated CPM-5 as a blue LED and luminescent sensor for selective Fe^{3+} sensing and temperature detection

Jian-Wei Zhang,*[a] Rui-Ying Yu,[a] Xi Li,[a] Hai-Qun Xu,[b] Jin-Hai Cui,[a] Xin-Cheng Hu[a] and Jie-Qiong Li*[a]

[a] School of Chemistry and Chemical Engineering, Shangqiu Normal University, Shangqiu, Henan, 476000, P. R. China.

[b] School of Food Science and Biotechnology, Zhejiang Gongshang University, Hangzhou 310038, P. R. China

***Corresponding Authors:**

E-mail for Jian-Wei Zhang: jwzhang85@163.com;

E-mail for Jie-Qiong Li: lijqchem@foxmail.com.

1. Materials and Methods.

All chemicals used in the syntheses were purchased from commercial sources and were used as received. TGA-DTA curves were performed on a NETZSCH STA 449F5 thermal analyzer in the range of 30-900 °C under nitrogen atmosphere. Powder X-ray diffraction (PXRD) pattern was collected by a Rigaku MiniFlex600 diffractometer with Cu Kα (λ =1.54056 Å). The crystal image and EDS-mapping of samples were performed by using Thermo Fisher Verios G4 equipped and its energy dispersive spectroscopy (EDS) detector. The UV-vis absorption spectra measured on a Hitachi U-3900 UV/vis spectrophotometer at room temperature The luminescence properties were recorded on Hitachi F-7100 fluorescence spectrophotometer at room temperature. The temperature-dependent luminescent measurements were recorded a Horiba FluoroMax+ spectrofluorometer. N_2 gas sorption/desorption isotherms at 77 K were measured on a Micromeritics ASAP 2020 Plus surface-area under low pressure.

2. Computational setup

All density functional theory calculations in this work were performed using the Gaussian 09 program suite.[S1] The equilibrium geometries were optimized at the Becke's three-parameter hybrid exchange functional combined with the Lee-Yang-Parr correlation functional (B3LYP).[S2,S3] With regard to the basis set, the "double-ζ" quality basis set consisting of the effective core potentials (LANL2DZ) of Hay and Wadt[S4,S5] was adopted for the In atom and the 6-31+G(*d*)[S6,S7] for all the non-metal atoms. A relativistic effective core potential (ECP) was employed to represent the core electrons of In atom. Vibrational frequencies were calculated at the same level to identify that each configuration is a minimum on the potential surface. The absorption spectra were simulated by TD-B3LYP calculations with the same basis set.[S8,S9]

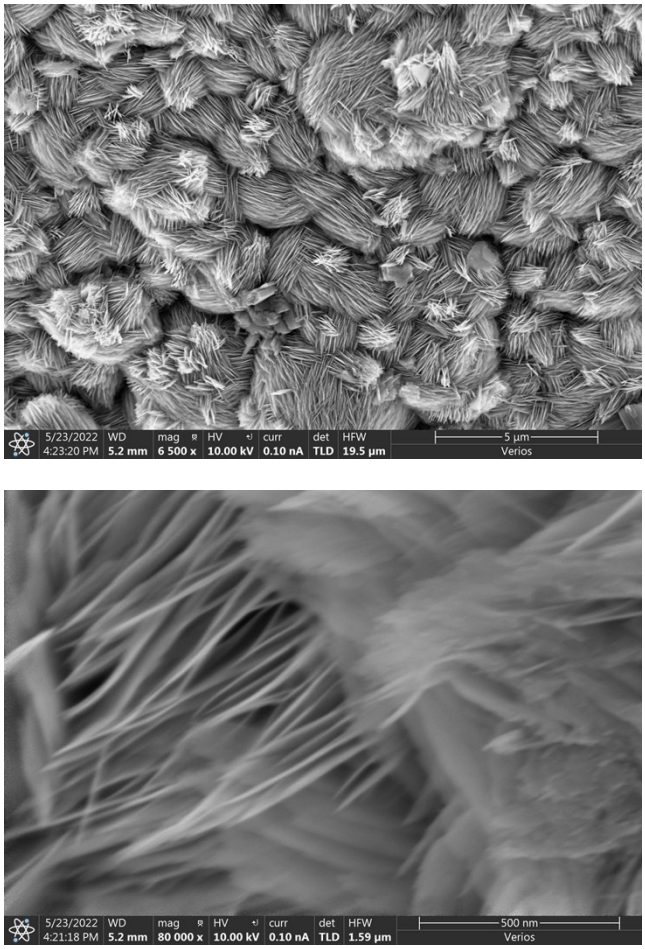

Fig. S1 SEM images of CPM-5-Cl.

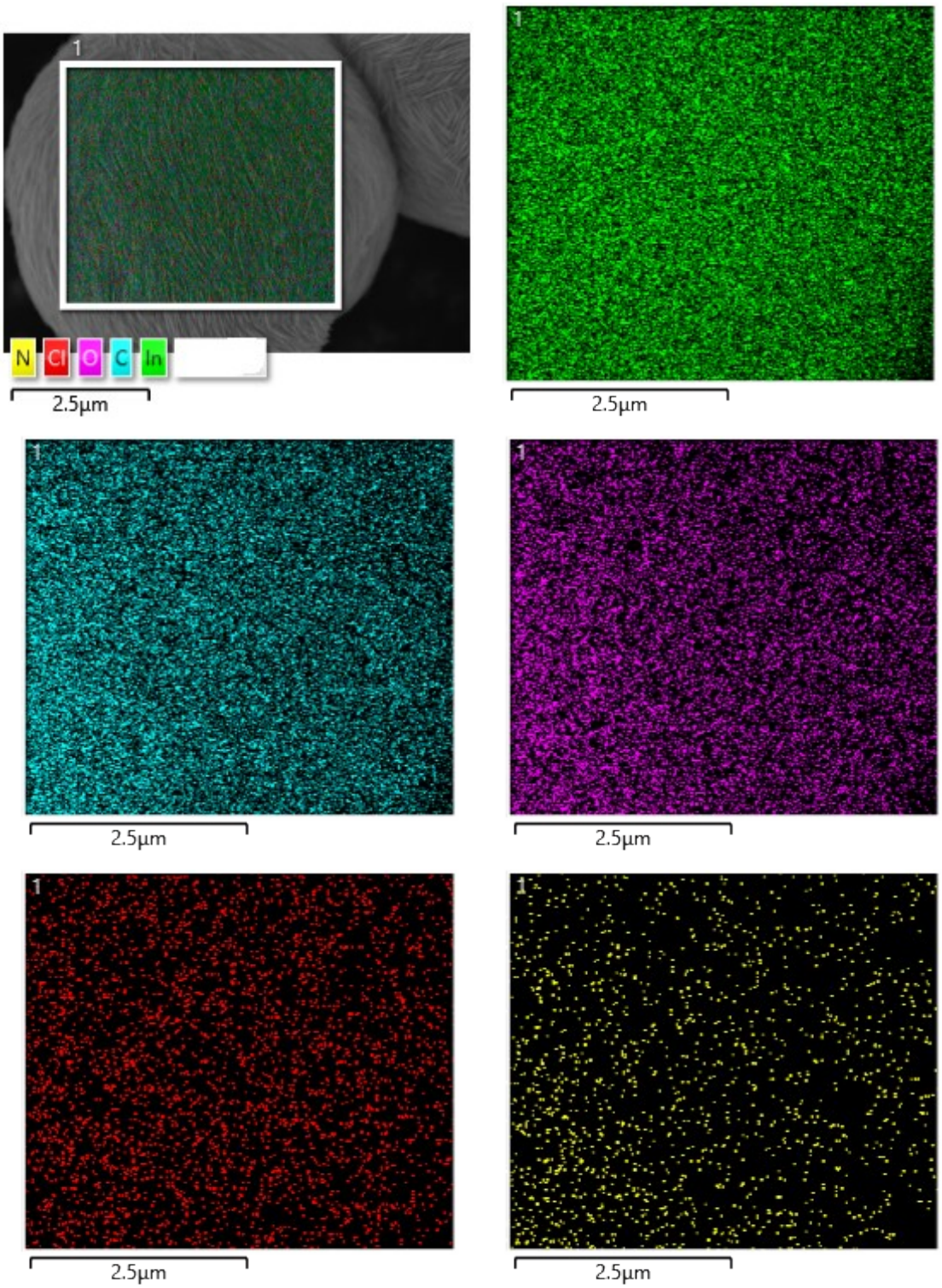

Fig. S2 EDS-mapping images of CPM-5-Cl.

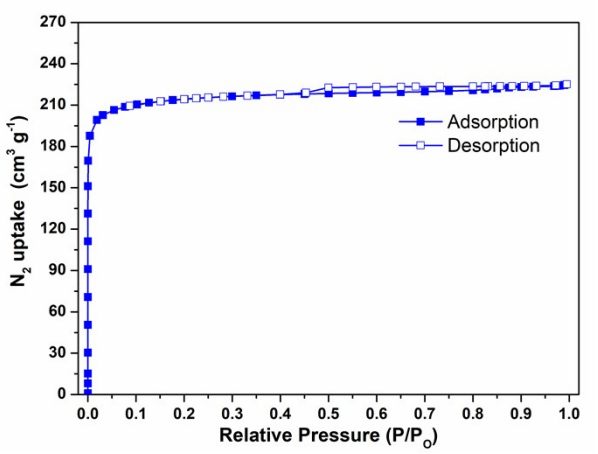

Fig. S3 Adsorption and desorption isotherms of N_2 at 77 K for CPM-5-Cl.

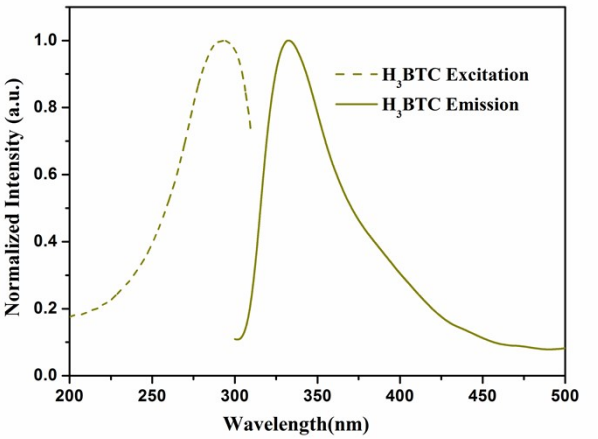

Fig. S4 Excitation and emission spectra of the free H_3BTC ligand.

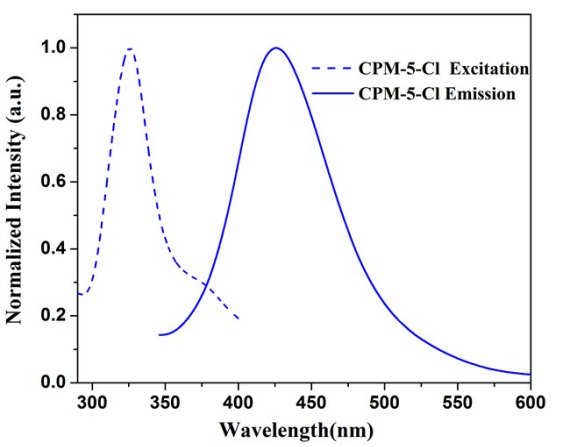

Fig. S5 Excitation and emission spectra of CPM-5-Cl.

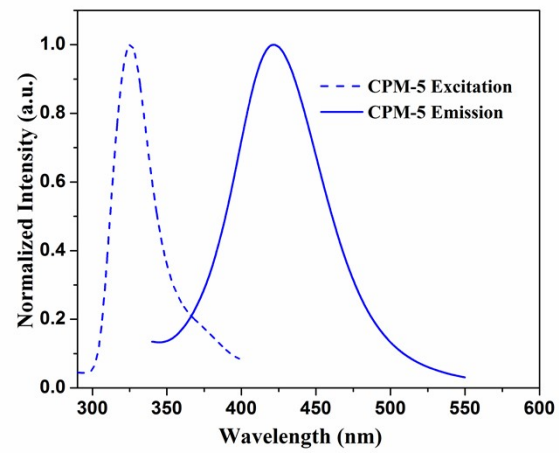

Fig. S6 Excitation and emission spectra of CPM-5.

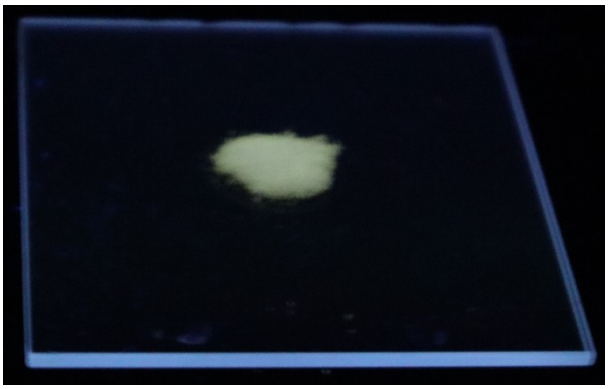

(a)

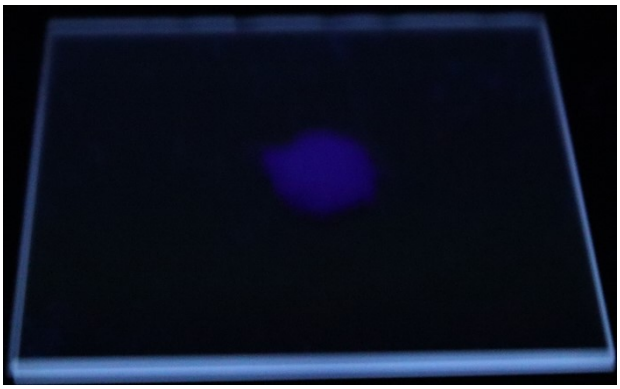

(b)

Fig. S7 Color changes from H_3BTC (a) to CPM-5-Cl (b) under UV 254 nm light.

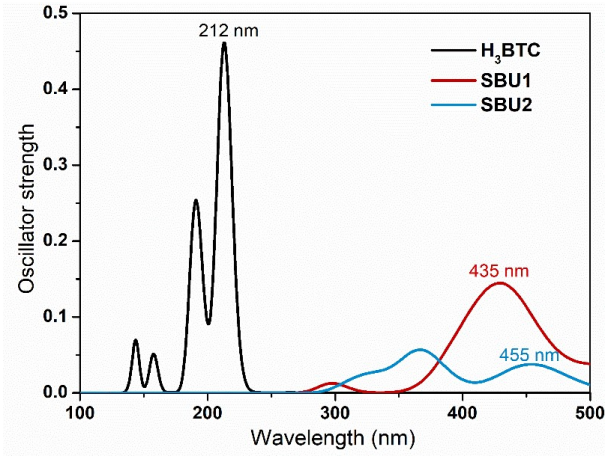

Fig. S8 Simulated adsorption spectra of **H_3BTC**, **SBU1** and **SBU2** at the TD-B3LYP/6-31+G(*d*)-LANL2DZ level of theory.

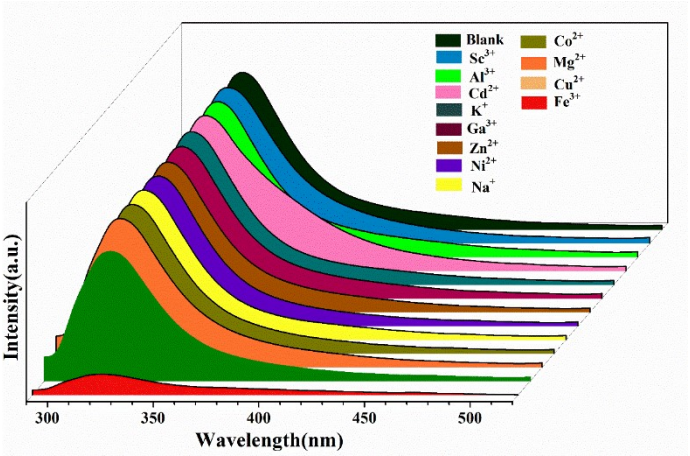

Fig. S9 Fluorescent spectra of CPM-5-Cl in the presence of 0.4 mM different metal ions under excitation of 270 nm.

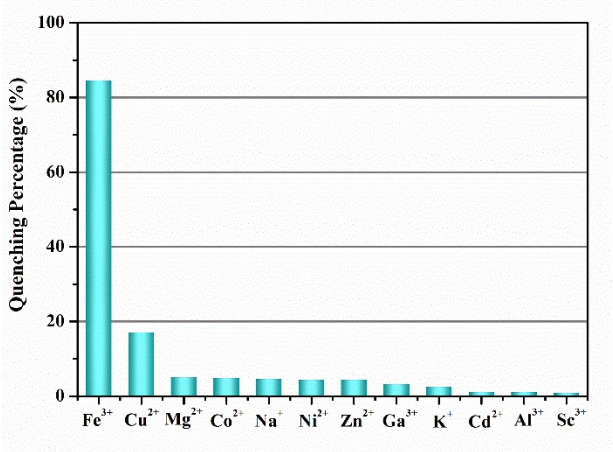

Fig. S10 Fluorescence quenching of CPM-5-Cl dispersed in aqueous solutions of twelve different metal cations (0.4 mM).

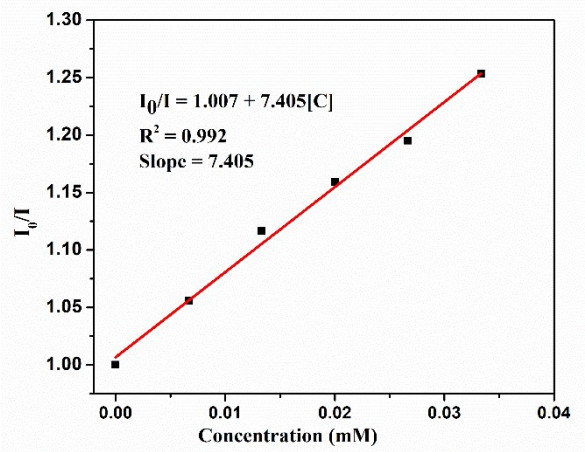

Fig. S11 Linearity relationship of luminescent intensity of CPM-5-Cl and Fe^{3+} ion at low concentrations.

Table S1. Comparison of maximum relative sensitivity (S_m, % K^{-1}) of reported ratiometric luminescent MOF thermometers with bimetallic Ln-MOFs.

Luminescent MOF	S_m (%K^{-1})	T_m (K)	Ref.
CPM-5-Cl	3.08	300	This work
$Eu_{0.37}Tb_{0.63}$-BTC-a	0.68	313	S10
$Nd_{0.577}Yb_{0.423}$BDC-F_4	1.2	313	S11
$Tb_{0.80}Eu_{0.20}$BPDA	1.19	313	S12
$Nd_{0.95}Yb_{0.05}$BPTC	0.94	293	S13
$Tb_{0.9}Eu_{0.1}$L	0.11	300	S14
$Tb_{0.99}Eu_{0.01}(BDC)_{1.5}$	0.31	318	S15
$Tb_{0.99}Eu_{0.01}$(pia)	2.75	300	S16

Table S2. Comparison of sensing performance of CPM-5-Cl for Fe^{3+} ion with other MOF-based materials.

Luminescent MOF	Solvent	K_{sv} (M^{-1})	Ref.
CPM-5-Cl	Water	7.405×10^3	This work
PCN-604	Water	8.53×10^3	S17
BUT-14	Water	2.17×10^3	S18
Cd-MDIP	Water	4.13×10^4	S19
Tb-DSOA	Water	3.54×10^3	S20
Eu-BPDA	Water	1.25×10^4	S21
Tb-MOF	Water	1.9×10^3	S22
Eu-MOF	Water	1.55×10^4	S23
Bi-MOF	Water	2.02×10^4	S24

References

S1 M. J. Frisch, G. W. Trucks, H. B. Schlegel, G. E. Scuseria, M. A. Robb, J. R. Cheeseman, G. Scalmani, V. Barone, B. Mennucci, G. A. Petersson, H. Nakatsuji, M. Caricato, X. Li, H. P. Hratchian, A. F. Izmaylov, J. Bloino, G. Zheng, J. L. Sonnenberg, M. Hada, M. Ehara, K. Toyota, R. Fukuda, J. Hasegawa, M. Ishida, T. Nakajima, Y. Honda, O. Kitao, H. Nakai, T. Vreven, J. A. Montgomery Jr., J. E. Peralta, F. Ogliaro, M. Bearpark, J. J. Heyd, E. Brothers, K. N. Kudin, V. N. Staroverov, R. Kobayashi, J. Normand, K. Raghavachari, A. Rendell, J. C. Burant, S. S. Iyengar, J. Tomasi, M. Cossi, N. Rega, J. M. Millam, M. Klene, J. E. Knox, J. B. Cross, V. Bakken, C. Adamo, J. Jaramillo, R. Gomperts, R. E. Stratmann, O. Yazyev, A. J. Austin, R. Cammi, C. Pomelli, J. W. Ochterski, R. L. Martin, K. Morokuma, V. G. Zakrzewski, G. A. Voth, P. Salvador, J. J. Dannenberg, S. Dapprich, A. D. Daniels, O. Farkas, J. B. Foresman, J. V. Ortiz, J. Cioslowski and D. J. Fox, Gaus-sian 09, Revision A.02, Gaussian, Inc., Wallingford CT, 2009.

S2 A. D. Becke, *J. Chem. Phys.*, 1993, **98**, 5648−5652.

S3 C. Lee, W. Yang and R. G. Parr, *Phys. Rev. B*, 1988, **37**, 785–789.

S4 P. J. Hay and W. R. Wadt, *J. Chem. Phys.*, 1985, **82**, 299–310.

S5 P. J. Hay and W. R. Wadt, *J. Chem. Phys.*, 1985, **82**, 270–283.

S6 W. J. Hehre, R. Ditchfield and J. A. Pople, *J. Chem. Phys.*, 1972, **56**, 2257–2261.

S7 M. J. Frisch, J. A. Pople and J. S. Binkley, *J. Chem. Phys.*, 1984, **80**, 3265–3269.

S8 T. Helgaker and P. Jo/rgensen, *J. Chem. Phys.*, 1991, **95**, 2595–2601.

S9 K. L. Bak, P. Jørgensen, T. Helgaker, K. Ruud and H. J. A. Jensen, *J. Chem. Phys.*, 1993, **98**, 8873–8887.

S10 H. Wang, D. Zhao, Y. Cui, Y. Yang and G. Qian, *J. Solid State Chem.*, 2017, **246**, 341–345.

S11 X. Lian, D. Zhao, Y. Cui, Y. Yang and G. Qian, *Chem. Commun.*, 2015,**51**, 17676–17679.

S12 D. Zhao, X. Rao, J. Yu, Y. Cui, Y. Yang and G. Qian, *Inorg. Chem.*, 2015, **54**, 11193–11199.

S13 C. Gu, Y. Y. Ding, X. H. Quan, M. Y. Gong, J. L. Yu, D. Zhao and C. Li, *J. Rare Earths.*, 2021, **39**, 1024–1030.

S14 S.-N. Zhao, L.-J. Li, X.-Z. Song, M. Zhu, Z.-M. Hao, X. Meng, L.-L. Wu, J. Feng, S.-Y. Song, C. Wang and H.-J. Zhang, *Adv. Funct. Mater.*, 2015, **25**, 1463–1469.

S15 A. Cadiau, C. D. S. Brites, P. M. F. J. Costa, R. A. S. Ferreira, J. Rocha and L. D. Carlos, *ACS Nano*, 2013, **7**, 7213–7218.

S16 X. Rao, T. Song, J. Gao, Y. Cui, Y. Yang, C. Wu, B. Chen and G. Qian, *J. Am Chem. Soc.*, 2013, **135**, 15559–15564.

S17 Y. Zhang, X. Yang and H.-C. Zhou, *Dalton Trans.*, 2018, **47**, 11806–11811.

S18 B. Wang, Q. Yang, C. Guo, Y. Sun, L. H. Xie and J. R. Li, *ACS Appl. Mater. Interfaces*, 2017, **9**, 10286–10295.

S19 Y. Li, Z. Chang, F. Huang, P. Wu, H. Chu and J. Wang, *Dalton Trans.*, 2018, **47**, 9267–9273.

S20 X.-Y. Dong, R. Wang, J.-Z. Wang, S.-Q. Zang and T. C. W. Mak, *J. Mater. Chem. A*, 2015*,* **3***,* 641–647.

S21 J. Wang, J. Wang, Y. Li, M. Jiang, L. Zhang and P. Wu, *New J. Chem.*, 2016*,* **40***,* 8600–8606.

S22 T. Jing, L. Chen, F. Jiang, Y. Yang, K. Zhou, M. Yu, Z. Cao, S. Li and M. Hong, *Cryst. Growth Des.*, 2018, **18**, 2956–2963.

S23 Y.-L. Gai, Q. Guo, X.-Y. Zhao, Y. Chen, S. Liu, Y. Zhang, C.-X. Zhuo, C. Yao and K.-C. Xiong, *Dalton Trans*., 2018, **47**, 12051–12055.

S24 Y. Sun, N. Zhang, Q. L. Guan, C. H. Liu, B. Li, K. Y. Zhang, G. H. Li, Y. H. Xing, F. Y. Bai and L. X. Sun, *Cryst. Growth Des.*, 2019, **19**, 7217–7229.